Electronic Supplementary Material (ESI) for New Journal of Chemistry.

A decatungstate-based Ionic liquid exhibiting very low dielectric constant suitable for acting as solvent and catalyst for oxidation of organic substrates

Yohan Martinetto,[a,b] Bruce Pégot,*[a] Catherine Roch,[a] Mohamed Haouas,[a]
Betty Cottyn-Boitte,[b] Franck Camerel,[c] Jelena Jeftic,[c] Denis Morineau,[d] Emmanuel Magnier,[a]
and Sébastien Floquet.*[a]

a. Institut Lavoisier de Versailles, UMR 8180, Université de Versailles St-Quentin en Yvelines, Université Paris-Saclay, 78035 Versailles, France.

b. Institut Jean-Pierre Bourgin, INRAE, Agro Paris Tech, Université Paris Saclay, 78000 Versailles, France.

c. Univ Rennes, CNRS, ISCR (Institut des Sciences Chimiques de Rennes) - UMR 6226, 35000 Rennes, France.

d. Institut de Physique de Rennes, UMR 6251, Université de Rennes 1, 35042 Rennes, France.

Corresponding authors: sebastien.floquet@uvsq.fr, bruce.pegot@uvsq.fr

Electronic Supporting Information

Table of contents:

Part 1: Experimental section

1. General methods

Fourier Transform Infrared (FT-IR) spectra were recorded on a 6700 FT-IR Nicolet spectrophotometer, using diamond ATR technique. The spectra were recorded on non-diluted compounds and ATR correction was applied.

ThermoGravimetric Analysis (TGA) analysis were recorded on a Seiko TG/DTA 320 thermogravimetric balance. The samples were measured between room temperature and 700 °C (scan rate: 5 °C.min^{-1}, under O_2).

Differential scanning calorimetry (DSC) was performed on a NETZSCH DSC 200 F3 instrument equipped with an N_2 cooler, allowing measurements from -170 °C up to 450 °C. The samples were examined at a scanning rate of 10°.min^{-1} by applying two heating and one cooling cycles. The apparatus was calibrated with indium (156.6 °C).

Ion Chromatography was performed on a 881 Compact IC pro Metrohm chromatograph using a column Metrosep A Supp 4 - 250/4.0 and a $NaHCO_3$ 4mM Na_2CO_3 1mM water / CH_3CN 75 : 25 mixture as eluant. The flow rate was set at 1mL / min and the temperature at 45°C.

Electrospray Ionization Mass Spectrometry (ESI-MS) spectra were collected using a Q-TOF instrument supplied by WATERS. Samples were solubilized in water at a concentration of 10^{-4} M and were introduced into the spectrometer via an ACQUITY UPLC WATERS system whilst a Leucine Enkephalin solution was co-injected via a micro pump as internal standard.

Energy-dispersive X-ray spectroscopy (EDX) measurements were performed on a JEOL JSM 5800LV apparatus.

Phase behavior was studied by **Polarized light Optical Microscopy** on a Nikon H600L polarizing microscope equipped with a Linkam “liquid crystal pro system” hotstage LTS420.

Viscosity measurements were performed on a Thermofischer Haake MARS III controlled-stress rheometer equipped with a cone-plate geometry (diameter = 35 mm, angle = 1°) and a Peltier thermal regulator.

Dielectric spectroscopy and conductivity were performed in the 0.1Hz-1Mhz frequency range. The data are recorded during the cooling of the sample from 70°C to -150°C. The sample was prepared in parallel plate geometry between two brass-plated electrodes with a diameter of 20 mm and a spacing of 60 μm maintained by Teflon spacers. The complex impedance of the as-prepared capacitor was measured with a Novocontrol high resolution dielectric Alpha analyzer with an active sample cell. The temperature of the sample was controlled by a Quatro temperature controller (Novocontrol) with nitrogen as a heating/cooling agent providing a temperature stability better than 0.1°C.

Nuclear magnetic resonance (NMR)

^{1}H (300 MHz) NMR, ^{13}C (75.5 Mhz) and ^{31}P (121.5 MHz) NMR spectra were recorded at room temperature on a Bruker AC-300 spectrometer in $(CD_3)_2CO$, CD_3OD and $(CD_3)_2SO$. Chemical shifts are reported in parts per million (ppm) relative to internal references. The residual peaks of $(CD_3)_2CO$ (2.05 ppm), CD_3OD (3.31 ppm) or $(CD_3)_2SO$ (2.5 ppm) for ^{1}H (300 MHz) NMR spectra.

Liquid ^{183}W NMR spectra of was obtained on a high resolution 400 MHz Bruker Avance spectrometer, equipped with 10 mm BBO probes. CD_3CN was used as a solvent. Spectra were measured in 10 mm tubes at a Larmor frequency of 16.7 MHz for the ^{183}W.

2. Syntheses and characterizations of POM-ILs

All reagents were purchased from commercial sources and used without further purification**.**

Synthesis of $TBA_4[W_{10}O_{32}]$. $TBA_4[W_{10}O_{32}]$ was synthetised as described in the literature.[1] **IR/cm^{-1}** (see Figure S1): 2955 (s), 2928 (vs), 2858 (s), 1469 (m), 1380 (w), 1162 (vw), 994 (vw), 958 (s), 891 (s), 805 (vs), 586 (w), 435 (m), 404 (m), 335 (w). **^{183}W NMR** (See Figure S4, Supporting Information) (16.7 MHz, CD_3CN): δ (ppm) -22.9 (s, 8W), -166 (s, 2W).

Synthesis of POM-IL $(P_{6,6,6,14})_4[W_{10}O_{32}]$: This synthesis was inspired from Fournier[1] In a 250 mL beaker flask sodium tungstate dihydrate (16 g, 50 mmol) was dissolved in 100 mL of boiling distilled water. Then 33.5 mL of boiling HCl (3 M) was added with a rapid stirring. After 2 minutes of strong boiling, tetradecyltrihexylphosphonium chloride ($P_{6,6,6,14}$,Cl) (7.55 g, 15 mmol) in 10 mL of ethanol was added. Polyoxometalate-based Ionic Liquid formed a dense phase in the bottom of the beaker. Finally, the aqueous phase was separated, and the POM-IL phase was washed 3 times with 40 mL of boiling distilled water and dried with a vacuum pump until the POM-IL became a clear blue-green viscous liquid. Yield 15 g, 72% based on tungstate. **IR/cm^{-1}** (see Figure S1): 2954 (s), 2926 (vs), 2855 (s), 1466 (m), 1408 (w), 1378 (w), 1212 (vw), 1112 (vw), 723 (m), 994 (vw), 958 (s), 891 (s), 805 (vs), 586 (w), 435 (m), 404 (m), 348 (vw), 335 (w). **^{1}H NMR** (See Figure S4) (300 MHz, $(CD_3)_2CO$): δ (ppm) 2.48 (m, 8H), 1.71 (m, 8H), 1.56 (m, 8H), 1.4-1.2 (m, 34H) and 0.88 (m, 12H). **^{31}P NMR** (121,5 MHz, $(CD_3)_2CO$): δ (ppm) 33,95. **^{183}W NMR** (See Figure S5) (16.7 MHz, (CD_3CN)): δ (ppm) -20.9 (s, 8W), -163 (s, 2W). **TGA** (see Figure S3): A weight loss of 39.4% between RT and 700 °C corresponds to a combustion of 4 cations $(P_{6,6,6,14})^+$ (expected 39.2 %) Thermogravimetric analyses show that the compound is stable up to 200 °C without any degradation and a total absence of water. **EDX** : no trace of Na and Cl coming from the tungstate or the phoshonium precursors detected. By **ion chromatography**, no trace of chloride ions has been detected. **ESI-MS** (CH_3CN, see Figure S2) : m/z 587.4 ($[W_{10}O_{32}]^{4-}$ expected m/z 587.6) and 783.8($[HW_{10}O_{32}]^{3-}$ expected m/z 783.8). **DSC**: The clear glass transition was centered around Tg = -10 °C.

Note that for this compound and other POM-ILs, an excess of $(P_{6,6,6,14})Cl$ can sometimes be identified by TGA, EDX and Ion chromatography experiments. TGA experiment is sensistive enough to get this information quickly. If so, the compound is dissolved in THF and passed through a steric exclusion gel column. The bigger species, *i.e*. the expected POM-IL, is not retained by the column and passes first. The $(P_{6,6,6,14})Cl$ in excess are smaller and are therefore retained by the gel. This technique allows to easily purify our POM-ILs. The purified compound is then dried under vacuum before characterization by FT-IR, TGA, Ion chromatography, EDX and so on.

Synthesis of $(P_{6,6,6,14})_2[W_6O_{19}]$: This synthesis was performed as described by Fournier.[2] A mixture of 16,5 g (50 mmol) of sodium tungstate dihydrate, 20 mL of acetic anhydride, and 15 mL of DMF is stirred in a 125 mL Erlenmeyer flask at 100 °C for 3 h. A solution of 10 mL of acetic anhydride and 9 mL of 12N HCl in 25 mL of DMF is added with stirring and the mixture is gravity filtered through a medium porosity filter paper in order to eliminate the undissolved white solid. After washing the solide with 25 mL of methanol, the clear filtrate is allowed to cool to room temperature. A solution of tetradecyltrihexylphosphonium chloride ($P_{6,6,6,14}$,Cl) (9.1 g, 18 mmol, 2.1 eq.) in 10 mL of ethanol was added. Polyoxometalate-based Ionic Liquid formed a dense phase in the bottom of the beaker. Finally, the organic phase was separated, and the POM-IL phase was dried with a vacuum pump until the POM-IL became a clear blue-green viscous liquid. Yield 1.5 g, 8% based on tungstate. **IR/cm^{-1}** (see Figure S1): 2955 (s), 2927 (vs), 2855 (s), 1465 (m), 1409 (w), 1378 (w), 1214 (vw), 1111 (vw), 723 (m), 978 (vs), 891 (vw), 815 (vs), 720 (w), 586 (m), 446 (s), 405 (vw), 368 (w). **^{183}W NMR** (See Figure S5) (16.7 MHz, (CD_3CN)): δ (ppm) 56 (s, 6W).

Part 2: Characterizations by FT-IR spectra

FT-IR spectra comparison of **$(P_{6,6,6,14})Cl$**, **$TBA_4[W_{10}O_{32}]$**, **$(P_{6,6,6,14})_4[W_{10}O_{32}]$** and **$(P_{6,6,6,14})_2[W_6O_{19}]$** are given in Figure S1.

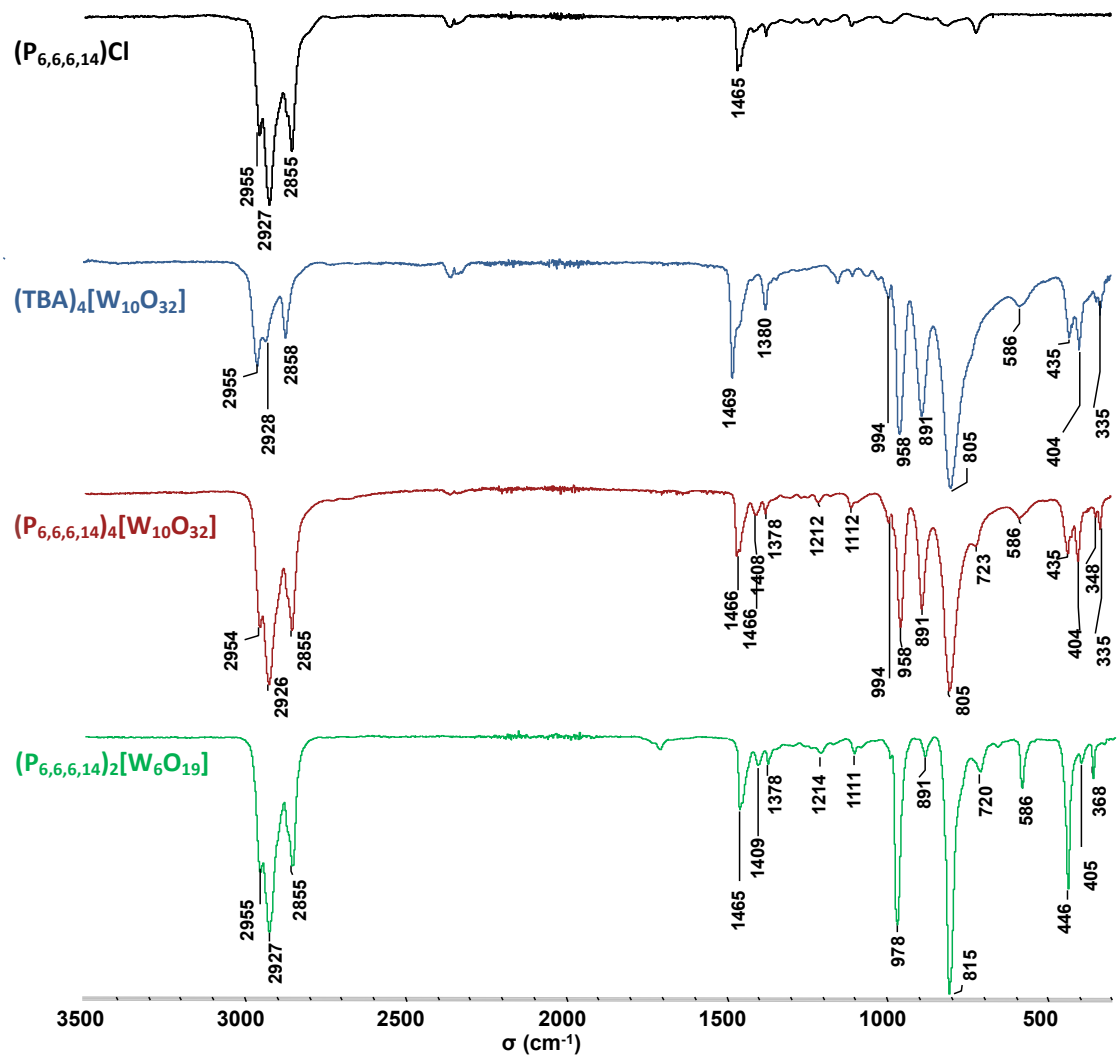

Figure S1: Infrared spectra comparing $(P_{6,6,6,14})_4[W_{10}O_{32}]$, $(P_{6,6,6,14})_2[W_6O_{19}]$, $(TBA)_4[W_{10}O_{32}]$ as reference and $(P_{6,6,6,14})Cl$.

All of the vibration bands between 3000 and 2850 cm^{-1} were assigned at the C-H aliphatic bonds.

- **$(P_{6,6,6,14})_4[W_{10}O_{32}]$**

In the FT-IR spectrum, the bands attributed to the $[W_{10}O_{32}]^{4-}$ are respectively : 958 cm^{-1} for W-O_t vibration and 891, 805 and 586 cm^{-1} for W-O_b-W and W-O_c-W vibration. These vibration bands are in agreement with literature[1] and the $TBA_4[W_{10}O_{32}]$ reference spectra.

- **$(P_{6,6,6,14})_2[W_6O_{19}]$**

The bands assigned to the $[W_6O_{19}]^{2-}$ are respectively : 978 cm^{-1} for W=O vibration and 815, and 446 cm^{-1} for W-O vibration. These vibration bands are in agreement with literature.[2]

Part 3: Characterizations by ESI-MS

The ESI-MS spectrum of compound $(P_{6,6,6,14})_4[W_{10}O_{32}]$ was recorded in CH_3CN in negative mode. As shown in Figure S2, the spectrum exibits two major peaks at m/z 587.4 and 783.8; which are attributed to the species $[W_{10}O_{32}]^{4-}$ (587.6) and $[HW_{10}O_{32}]^{3-}$ (783.8), respectively. It confirms the nature of the POM in the compound $(P_{6,6,6,14})_4[W_{10}O_{32}]$. Note that the peak found at m/z 703.8 is attributed to the formation of $[W_6O_{19}]^{2-}$ generated during the ESI-MS experiment. This assumption is confirmed by the fact that by increasing the cone voltage of the experiment this peak becomes predominant.

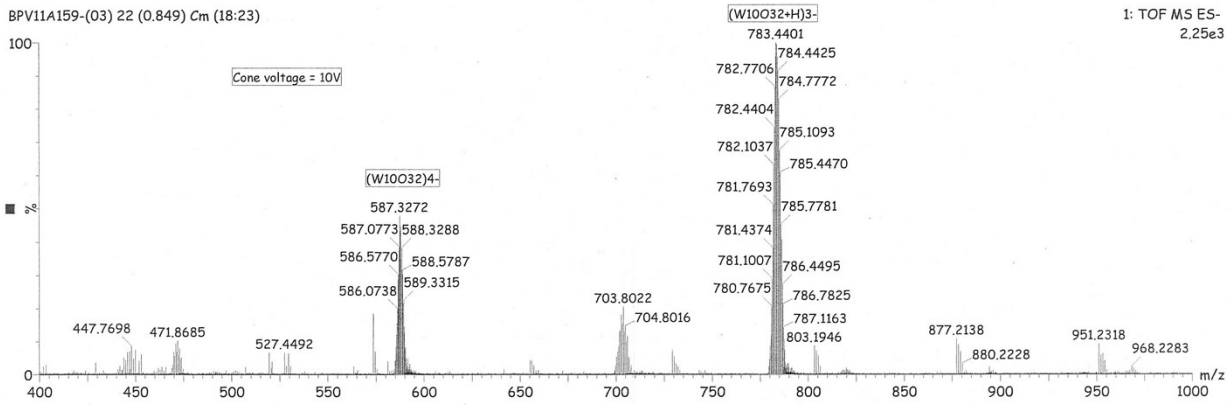

Figure S2: ESI-MS spectrum of $(P_{6,6,6,14})_4[W_{10}O_{32}]$ in CH_3CN in negative mode.

Part 4: ThermoGravimetric Analysis (TGA)

The TGA experiment is fully informative for the characterization of POM-ILs. Considering that under O_2 the compounds are burned into WO_3 and P_2O_5 above 600°C and that all the organic parts and eventually chloride ions coming from an excess of $(P_{6,6,6,14})Cl$ are removed during the TGA experiments.

As examplified below, we can easily distinguish samples with an excess of $(P_{6,6,6,14})Cl$. In Figure S3a, the TGA curve recorded for a POM-IL indicates a weight loss of 47%, which fully agree with the formula $(P_{6,6,6,14})_4[W_{10}O_{32}].((P_{6,6,6,14})Cl)_{1.6}$. EDX measurement confirms the presence of chloride in excess in the same order. In this case, the compound can be purified by passing THF solution of the compound on steric exclusion gel column until the TGA agrees with the expected weight loss (Figure S3b, which exactly corresponds to the weight loss expected for $(P_{6,6,6,14})_4[W_{10}O_{32}]$.(calculated 39.2%). The purity, and the absence of supplementary $(P_{6,6,6,14})Cl$ salt is confirmed by EDX and by ion chromatography.

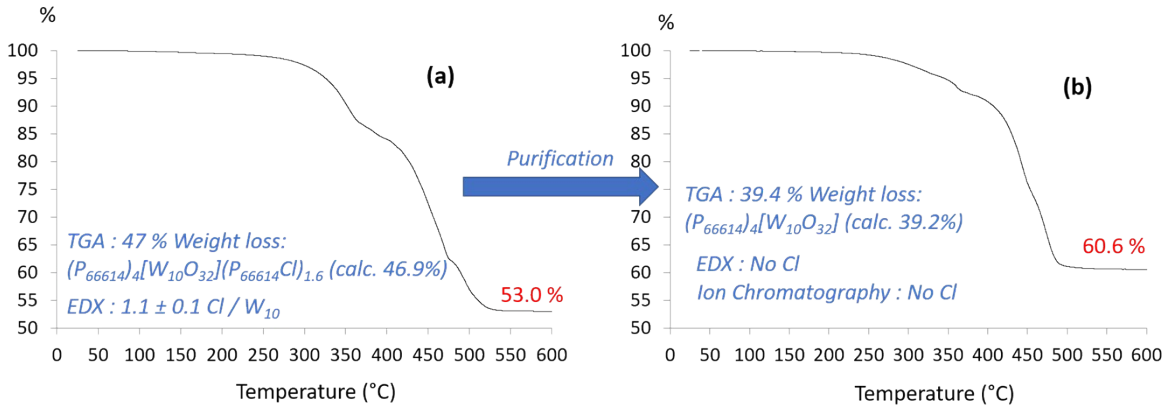

Figure S3: ThermoGravimetric curve of $(P_{6,6,6,14})_4[W_{10}O_{32}]$ recorded under oxygen at 5 °C/minute.

The TGA curve under oxygen flow confirms the absence of water solvate in the POM-IL due to the missing mass drop around 100 °C. We can also propose an approximate value of decomposition around 200 °C.

A final weight of 60.6% perfectly matches with the combustion of the organic part of the 4 organic cations $(P_{6,6,6,14})^+$ for yielding at the end P_2O_5 and WO_3.

Part 5: NMR studies in solution

1- ^{1}H NMR: Characterization of $(P_{6,6,6,14})_4[W_{10}O_{32}]$ comparing to $(P_{6,6,6,14})Cl$ in $(CD_3)_2CO$.

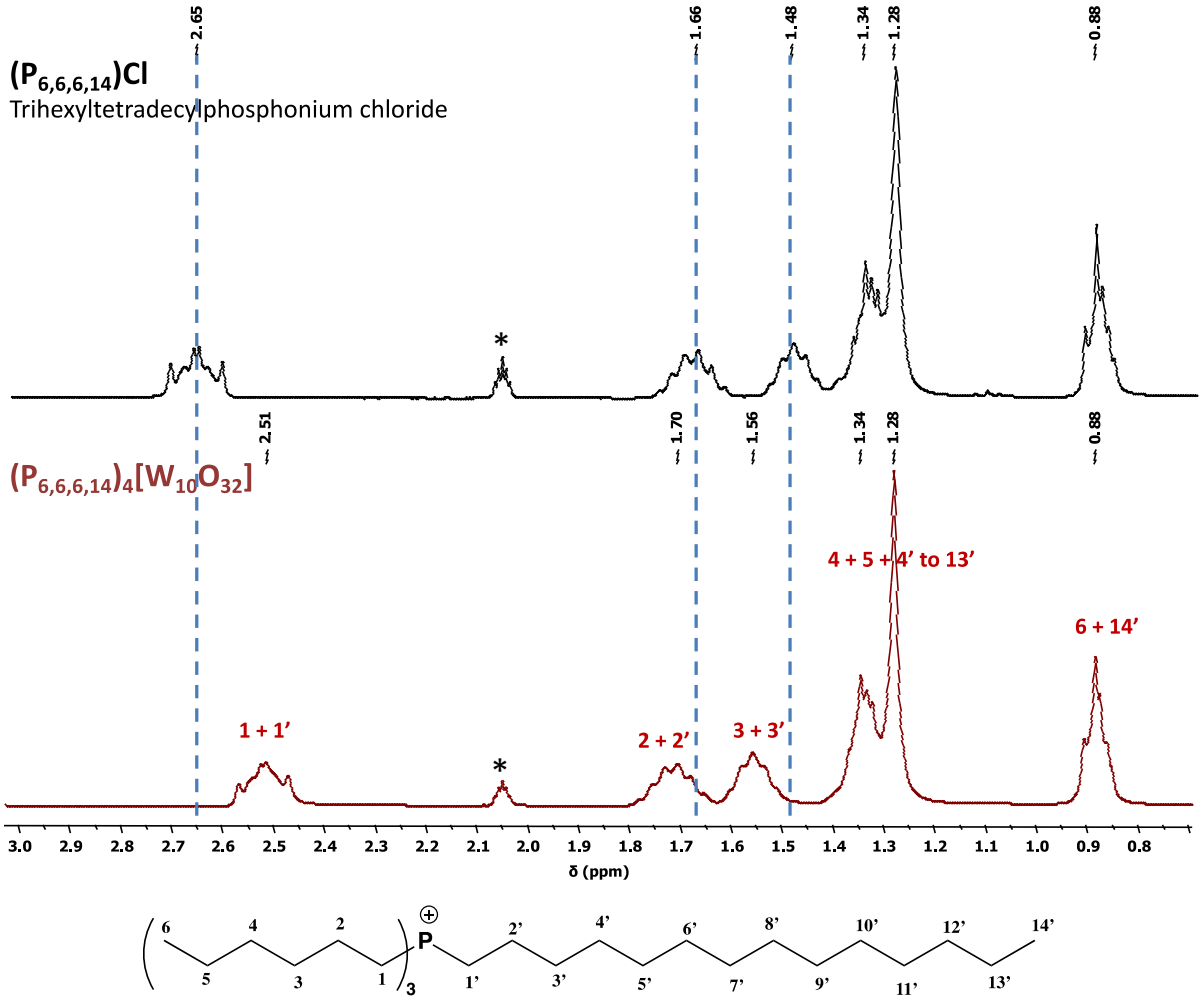

*Figure S4: ^{1}H NMR spectra comparing $(P_{6,6,6,14})_4[W_{10}O_{32}]$and $(P_{6,6,6,14})Cl$ and peaks' attibution. * indicate the signal attributed to $(CD_3)_2CO$*

The ^{1}H NMR spectra indicate significant shifts in both directions of the methylenic protons (2.51 ppm, 1.70 ppm and 1.56 ppm) which are closest from the phosphorus atom. This gap suggests a strong interaction between the POM and cations.

2- ^{13}C NMR: Characterization of $(P_{6,6,6,14})_4[W_{10}O_{32}]$ in $(CD_3)_2CO$.

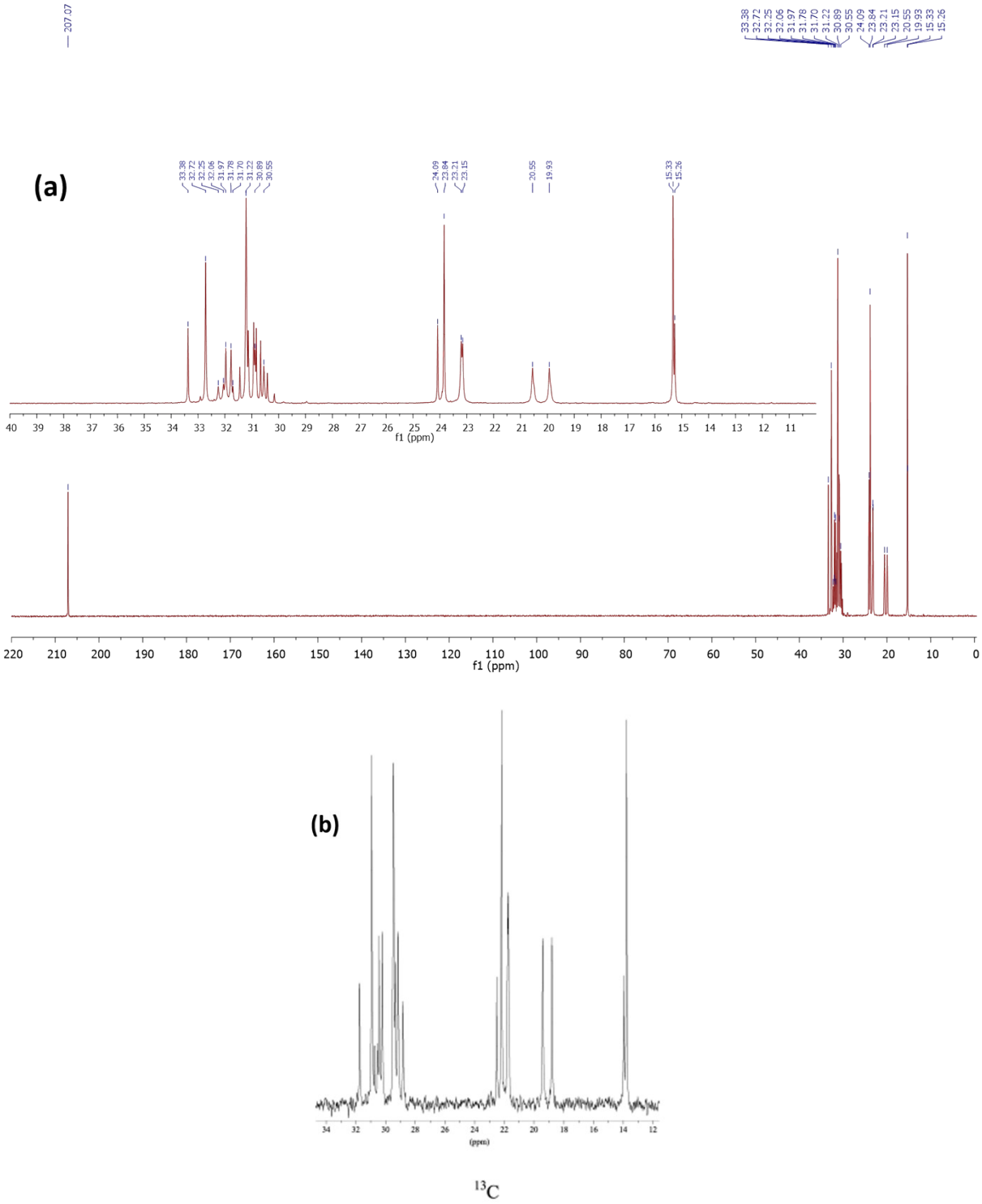

Figure S5: ^{13}C NMR spectra of $(P_{6,6,6,14})_4[W_{10}O_{32}]$ in $(CD_3)_2CO$ (a) in comparison with that of $(P_{6,6,6,14})Cl$ in $CDCl_3$.[3]

3- ^{183}W NMR (16.7 MHz, CD_3CN): NMR spectra comparing $(P_{6,6,6,14})_4[W_{10}O_{32}]$, $(P_{6,6,6,14})_2[W_6O_{19}]$ and $(TBA)_4[W_{10}O_{32}]$.

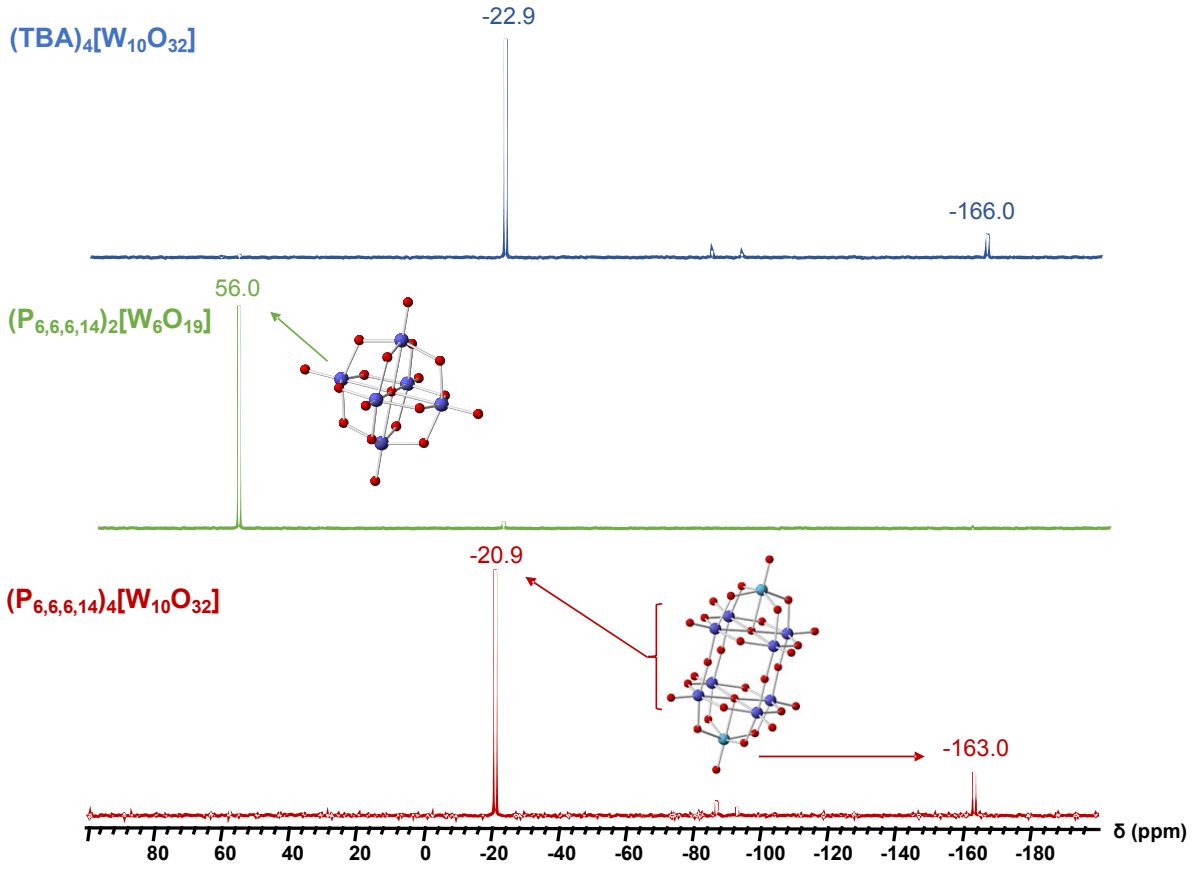

Figure S6: ^{183}W NMR (16.7 MHz, CD_3CN) spectra comparing $(P_{6,6,6,14})_4[W_{10}O_{32}]$, $(P_{6,6,6,14})_2[W_6O_{19}]$ and $(TBA)_4[W_{10}O_{32}]$.

The ^{183}W NMR spectrum of **$(P_{6,6,6,14})_4[W_{10}O_{32}]$** shows two peaks around -21 and -163 ppm with a 4: 1 intensity ratio, which correspond to two expected types of tungsten atoms, equatorial and capped, in the $[W_{10}O_{32}]^{4-}$ structure reported in the literature as TBA salt.[4] For $[W_6O_{19}]^{2-}$, the highly symmetrical Lindqvist anion produce a single pic at 56 ppm in ^{183}W NMR and confirms its formation.[5] No trace of $[W_6O_{19}]^{2-}$ was observed in the spectrum of $(P_{6,6,6,14})_4[W_{10}O_{32}]$.

Part 6: Rheological analyses

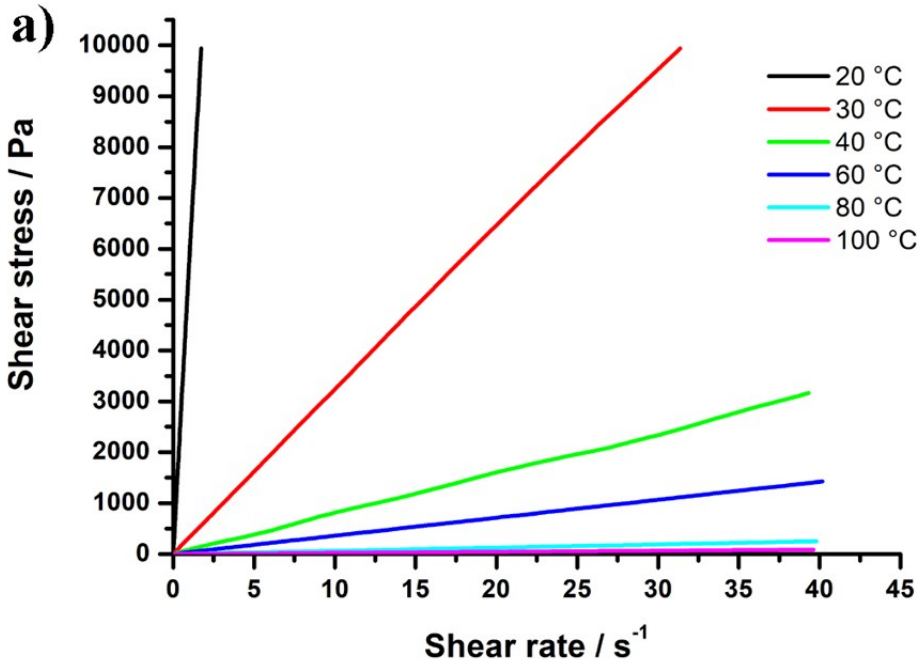

Figure S7: Analysis of $(P_{6,6,6,14})_4[W_{10}O_{32}]$. a) Flow curves $\tau = f(\dot{\gamma})$ showing the evolutions of the shear stress versus the shear rate at various temperatures for this compound. Each line corresponds to a curve $\tau = f(\dot{\gamma})$ for a given temperature;

Conductivity of $(P_{6,6,6,14})_4[W_{10}O_{32}]$.

The dielectric loss as a function of the frequency for a wide range of studied temperatures are shown in Figures S8 and S9 The temperature step between each curve is 5 °C. For the highest temperature T = 70 °C (upper curve), the intensity of the dielectric loss is dominated by ionic conductivity. The signal flattens at lower temperature and the dipolar relaxation modes show up on cooling down to the lowest studied temperature -150 °C (lower curve), as also shown in Figure S9.

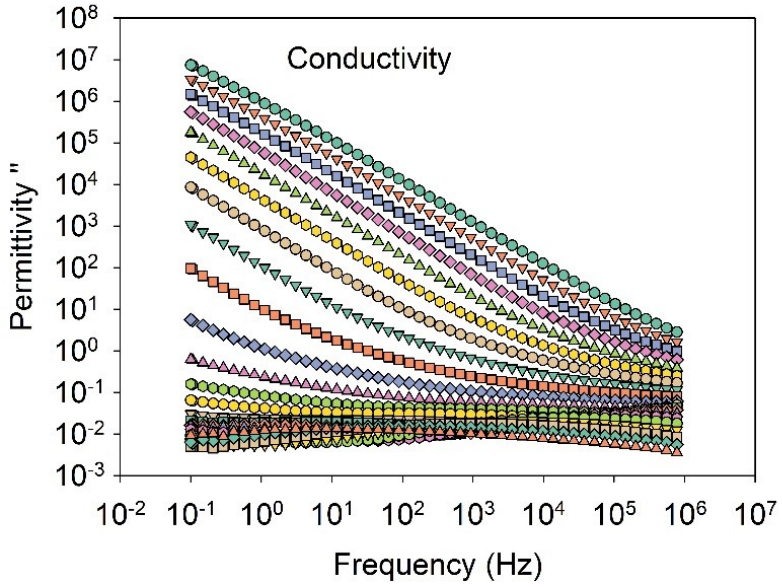

Figure S8: Dielectric loss as a function of the frequency at regularly spaced temperatures ranging from T = 70 °C (upper curve) to -150 °C (lower curve).

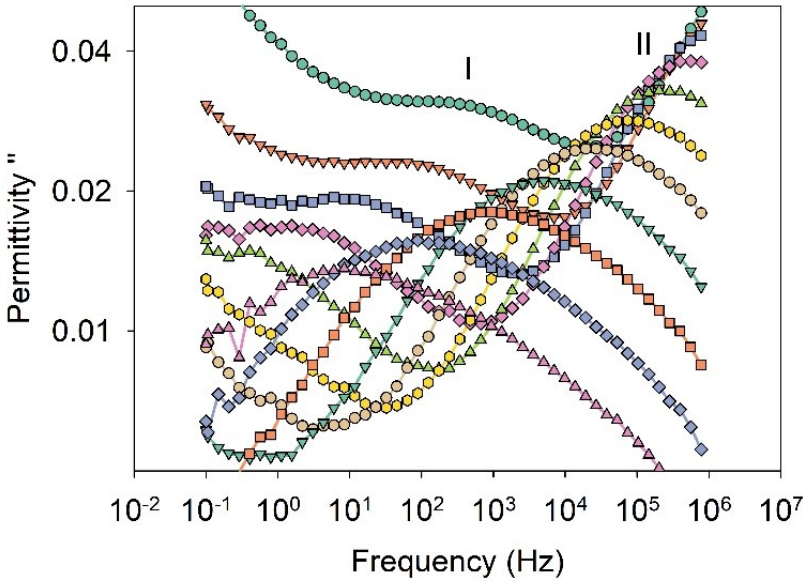

Figure S9: Magnified plot of the dielectric loss as a function of the frequency in the region of low temperatures from T = -50 °C (upper curve) to -150 °C (lower curve).

The ionic conductivity may be related to the diffusion coefficient through the Nernst-Einstein equation $\sigma_0 = \frac{ne^2D}{kT}$, where *n* is the number density of charge carriers, *e* is the electric charge and *k* is Boltzmann's constant. In addition, the diffusion coefficient may be related to the viscosity η through the Stoke-Einstein equation $D = \frac{kT}{6\pi a\eta}$, where *a* is the hydrodynamic radius of the diffusion particles. If both equations apply, the conductivity is in turn inversely

proportional to the viscosity. This relation between conductivity and viscosity was actually confirmed, as shown in Figure S10, where both quantities are plotted as a function of the inverse temperature. In the temperature range above room temperature where both quantities were measured, they fulfill an Arrhenius law with a comparable value of the activation energy (85 ± 5 kJ.mole^{-1}). At lower temperature, one noticed a deviation of the inverse conductivity, which exhibits a super-Arrhenius behavior. This apparent increase of the activation energy is typically observed in glassforming liquids and commonly attributed to the onset of dynamical cooperativity in fragile liquids at low temperature under supercooling conditions.[6]

The two relaxation modes exhibit significantly smaller activation energies (57 and 32 kJ.mole^{-1} for the mode I and II respectively), and a Arrhenius-like behaviour. This suggest that, unlike conductivity, these modes are decoupled from the hydrodynamic viscosity.[7] They are more likely attributed to local rearrangements, usually named beta-processes, that induce polarization fluctuations, such as ligands tumbling or POM–ligand breathing modes. This hypothesis is comforted by the small values of the dielectric strength of the two modes ($0.1 < \Delta\varepsilon_{1,2} < 0.2$), in agreement with the overall spherical symmetry of the POM and very weakly polar character of the ligands.

It is commonly observed for glassforming liquids that the extrapolation of the main structural relaxation time reaches values of the order of 10^2 s at the calorimetric glass transition temperature Tg.[8,9] Universal scaling of conductivity, viscosity and the main structural relaxation were also observed for series of ionic liquids.[8] Although the present liquid also demonstrates a coupling between conductivity and viscosity, it is noteworthy that the two dielectrically active relaxation modes extrapolate to 10^2 s for tempartures that are far below the calorimetric Tg. This further confirms that they correspond to secondary (beta) processes. The experimental detection of an electrically active mode associated with the main (alpha) relaxation was presumably hidden due to the strong contribution of superimposed conductivity.

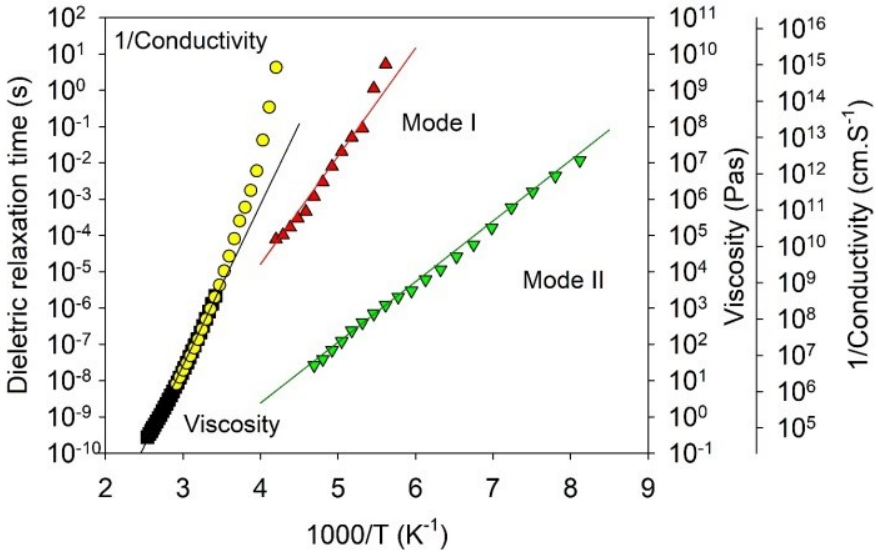

Figure S10: Arrhenius plot of the inverse conductivity (circles), dielectric relaxation time of the mode I (upward triangles) and mode II (downward triangles), and viscosity (squares). Solid lines are Arrhenius fits to the data.

Part 7: Catalysis experiments

All chemicals were purchased at high level of purity from Sigma–Aldrich, ABCR , Apollo Scientific. or Alfa Aesar companies and were used without further purification. Organic solvents were purchased from Merck and Carlo Erba.

1- Experimental procedure for oxidation of alcohols.

The experimental procedure used for catalysis is depicted in scheme S1 below, while Table S1 give some optimization reaction leading to the protocol wh chose to use for this study.

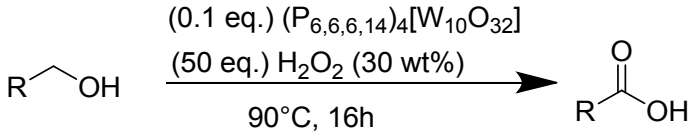

Scheme S1: General equation reaction of oxidation of alcohols

Table S1: optimisation and test reactions.

Entry [a]	Catalyst $(P_{6,6,6,14})_4[W_{10}O_{32}]$	H_2O_2 30% W	Time (h)	Conversion (%)[a]	Aldehyde yield (%)[a]	Acid yield (%)[a]
1 [b]	0.1 eq.	50 eq.	1	88	24	56
2	0.1 eq.	50 eq.	16	100	/	98 (93)[b]
3[c]	0.1 eq.	0 eq.	16	4	<1	<1

4	0 eq.	50 eq.	16	15	<1	10

[a]determined by ^{19}F NMR analysis using trifluoroanisol as internal standard. [b]Isolated yield after product separation from POM-IL phase by a reusable steric polymer column.

Protocol followed for this study : In a 100 mL flask equipped with condenser 1 eq. of alcohol (4-fluorobenzyl alcohol 2 mmmol, 252mg) and 0.1 eq. of catalyst ($(P_{6,6,6,14})_4[W_{10}O_{32}]$, 0.1mmol, 0.858g) were introduced. The mixture was stirred during a few minutes at 90 °C and then hydrogen peroxide (30 wt% in water) (50 eq., 7.8ml) were quickly added. This biphasic system was kept at 90°C for 16 h. The biphasic mixtures were then cooled at room temperature and separated by decantation after addition of 20 mL of distilled water. The aqueous phase was extracted 3 times with 20 mL of diethyl ether and the organic phase obtained was dried over $MgSO_4$ and concentrated under reduced pressure. Considering the ionic liquid phase, acetone was added until a homogenous phase was obtained (around 20 mL). The solution was dried over $MgSO_4$ and concentrated under reduced pressure. These two collected organic phases were mixed, and a minimum of tetrahydrofuran was added until a clear solution was obtained. The catalyst was then separated from the reactions products by a reusable steric exclusion polymer column composed of poly(styrene-co-divinylbenzene) eluted by tetrahydrofuran (around 100 mL). the POM-IL, was firstly recovered and after evaporation of THF the catalyst could be directly reused in an other cycle. The oxidation products are isolated secondly from the column to give 4-fluorobenzoic acid in 93% isolated yield (0.186mmol, 261mg). Purification of reaction products, when necessary, was performed by recrystallization, pentane washing or silica plate. All data (NMR ^1H, IR) of the synthetized product are in accordance with aldrich commercially available componds and their analytical documents (see Aldrich website) and purity is the limite of NMR détection.

2- Reference reactions

To evidence the catalytic activity of $(P_{6,6,6,14})_4[W_{10}O_{32}]$, number of reference reactions were performed. The experimental conditions are given in Tables S2 and S3.

Table S2: Table of verification reactions, general protocol with different catalysts and conditions.

Entry	Catalyst	H_2O_2	Aldehyde yield (%)	Acid Yield (%)
1	No catalyst	50 eq	<1	10[c]
2	$(P_{6,6,6,14})_4Cl$	50 eq.	7	23[c]
3[b]	$(P_{6,6,6,14})_4[W_{10}O_{32}]$	None	<1	<1[c]
4	$(P_{6,6,6,14})_4[W_{10}O_{32}]$	50 eq.	/	93[d]
5[e]	$TBA_4[W_{10}O_{32}]$	50 eq.	<1	65[c]

[a]Reaction conditions: 4-fluorobenzyl alcohol (1 eq.), H_2O_2 30 wt% (50 eq.), catalyst (0.1 eq.), 90°C, overnight.[b]Reaction conditions: 4-fluorobenzyl alcohol (1 eq.), without H_2O_2, catalyst (0.1 eq.), 90°C, overnight.[c]None isolated yield, detected by ^{19}F NMR analysis.[d]Isolated yield after catalyst/product separation by a reusable steric polymer column and purification by pentane washing.[e] Catalyst not recover, and isolation of product very complexe.

Table S3: Reactivity comparison between $(P_{6,6,6,14})_4[W_{10}O_{32}]$ and $(P_{6,6,6,14})_2[W_6O_{19}]$.

Entry	Catalyst	Alcohol conversion (%)[b]	Unknow product (%)[b]	Aldehyde (%)[b]	Acid (%)[b]
1	$(P_{6,6,6,14})_2[W_6O_{19}]$	77	20	24	26
2	$(P_{6,6,6,14})_4[W_{10}O_{32}]$	100	19	24	56

[a]Reaction conditions: 4-fluorobenzyl alcohol (1 eq.), H_2O_2 30 wt% (50 eq.), catalyst (0.1 eq.), 90 °C, 2 h.
[b]None isolated yield, only detected by ^{19}F NMR analysis.

The Table S2 collects data from different verifications reactions tested. We can see in Entry 1 a reaction without catalyst didn't work well. Entry 2 a reaction without $[W_{10}O_{32}]^{4-}$, give very poor yield. Entry 3 a reaction without H_2O_2 : without oxydant unsurprisingly only starting material was observed. Entry 4 the "classical" reaction in POM-IL medium in presence of H_2O_2 give very good isolated yield and the catalyst could be recoverd and reused. And Entry 5 with solide salt $TBA_4[W_{10}O_{32}]$, moderate yield was observed, but catalyst couldn't be recoverd and experimental procedure to isolate the product is complex and unsatisfactory compared to NMR yield. This table demonstrates that the couple $(P_{6,6,6,14})_4[W_{10}O_{32}]$ / H_2O_2 is needed to observe catalysis with a good yield.

Besides, the Table S3, demonstrates that of $(P_{6,6,6,14})_2[W_6O_{19}]$ is less efficient than $(P_{6,6,6,14})_4[W_{10}O_{32}]$, which explains the decrease of the yield after several runs, concomitantly with the formation of $(P_{6,6,6,14})_2[W_6O_{19}]$ (vide infra).

3- Recyclability tests of catalyst and analysis after catalysis

The integrity of the catalyst after catalytic process was checked by ^{183}W NMR (Figure S9). The ^{183}W NMR spectrum after 5 runs shows the $(P_{6,6,6,14})_4[W_{10}O_{32}]$ POM is maintained while a minor quantity of $(P_{6,6,6,14})_2[W_6O_{19}]$ linqvist POM (around 21 % after 5 runs) appears, in agreement with the decrease of the catalytic yield (*vide supra*).

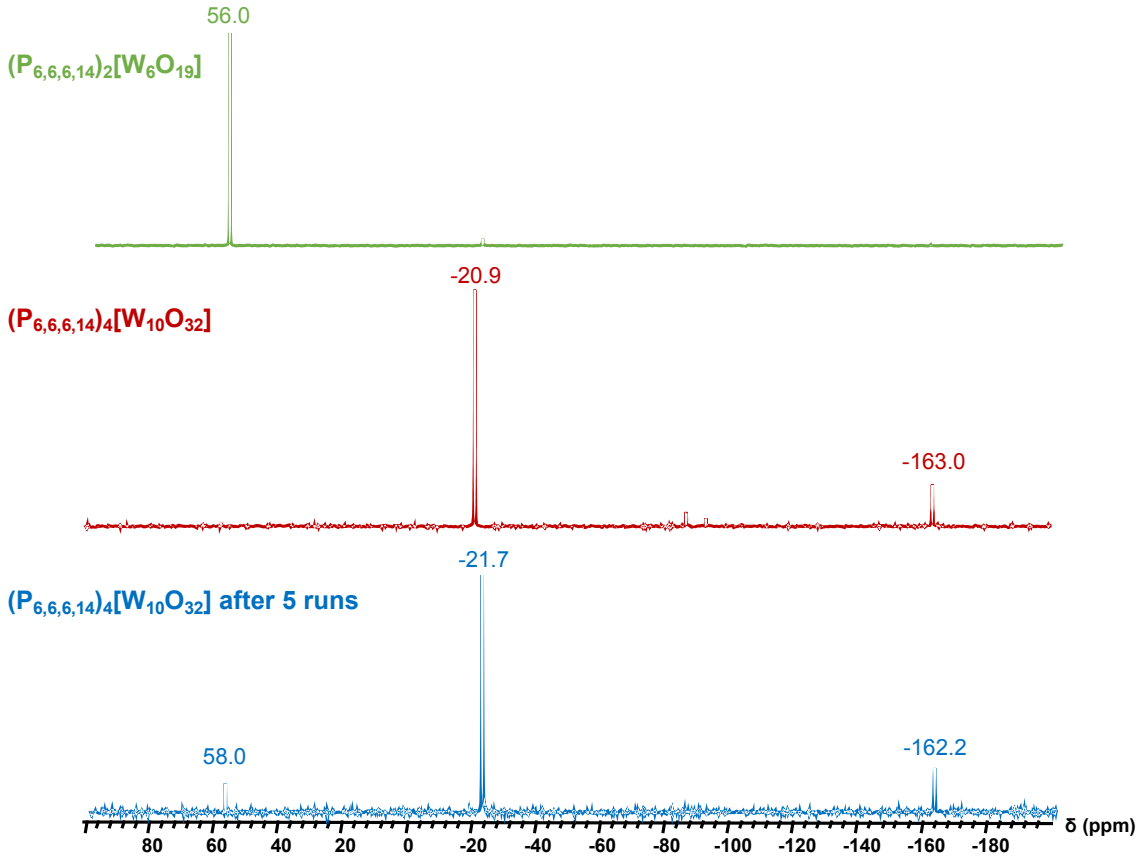

Figure S11: ^{183}W NMR (16.7 MHz, CD_3CN) spectra comparing $(P_{6,6,6,14})_4[W_{10}O_{32}]$ after 5 runs of catalysis, initial $(P_{6,6,6,14})_4[W_{10}O_{32}]$ and $(P_{6,6,6,14})_2[W_6O_{19}]$.

References

(1) Founier, M. *Inorganic Syntheses, 1990, Vol. 27*; 81

(2) Founier, M. *Inorganic Syntheses, 1990, Vol. 27*; 80.

(3) Bradaric, C.J., Downard, A. Kennedy, C., Robertson A.J., Zhou **Y.,** *Green Chemistry*, 2003, 5, 143–152

(4) Yamase, T.; Usami, T. *J. CHEM. SOC. DALTON TRANS.* **1988**, 8.

(5) Inoue, M.; Yamase, T.; Kazansky, L. P., *Polyhedron* **2003**, *22* (9), 1183–1189. https://doi.org/10.1016/S0277-5387(03)00119-0.

(6) Ediger, M. D.; Angell, C. A.; Nagel, S. R. Supercooled Liquids and Glasses. 13.

(7) Krause, C.; Yin, H.; Cerclier, C.; Morineau, D.; Wurm, A.; Schick, C.; Emmerling, F.; Schönhals, *Soft Matter* **2012**, *8* (43), 11115. https://doi.org/10.1039/c2sm25610j.

(8) Sangoro J. R., Kremer F., ACCOUNTS OF CHEMICAL RESEARCH **2012,** 45 (4), 4525–532.

(9) Wojnarowska Z. and Paluch M. J. Phys.: Condens. Matter **2015,** 27, 073202